THEORETICAL STUDY OF RADIANT HEAT EXCHANGE FOR NON-GRAY NON-DIFFUSE SURFACES IN A SPACE ENVIRONMENT

NASA Research grant: No. NGR-14-005-036

University of Illinois Budget Code: 46-22-40-356

Semi-Annual Status Report Number 3

Period Covered: February 1966 to July 1966

Prepared by: R. G. Hering
A. F. Houchens
T. F. Smith

Submitted by: R. G. Hering
Associate Professor of
Mechanical Engineering
266 Mechanical Engineering Building
University of Illinois, Urbana, Illinois
Phone: Area Code 217, 333-0366

Date: July 1, 1966

GPO PRICE $ _____

CFSTI PRICE(S) $ _____

Hard copy (HC) 2.00

Microfiche (MF) .50

ff 653 July 65

FACILITY FORM 602

N66 32438 (ACCESSION NUMBER)

(THRU)

37 (PAGES)

1 (CODE)

CR-76764 (NASA CR OR TMX OR AD NUMBER)

33 (CATEGORY)

TABLE OF CONTENTS

		page
	Nomenclature	iii
1.	OBJECTIVES AND SCOPE	1
2.	CURRENT STATUS	1
	2.1 Radiant Heat Exchange for Non-Gray, Non-Diffuse Surfaces in a Space Environment	1
	2.2 Radiant Heat Exchange for Gray Diffuse Surfaces in a Space Environment	3
	2.3 Radiant Heat Exchange Between Specularly Reflecting Surfaces with Direction Dependent Properties	9
	2.4 Radiation Properties for Rough Surfaces of Conducting Materials	10
	2.5 Radiation Properties for Optically Smooth Plane Surfaces	10
3.	PROPOSED FUTURE RESEARCH	13
4.	REFERENCES	15
5.	FIGURES	16
6.	APPENDIX - MANUSCRIPT OF TECHNICAL PAPER	24
7.	EXPENDITURES	32

NOMENCLATURE

dA_i	-	differential area of plate i
a	-	correlation distance
a_o	-	geometry dimension
$B(x_i)$	-	radiosity at x_i
b_o	-	geometry dimension
C_λ	-	coefficients as defined in Equation (2.1.1)
C_i	-	coefficients for plate i as defined in Equation (2.2.7) and Equation (2.2.8)
$E(x_i)$	-	emissive power at x_i
G_i	-	coefficients for plate i as defined in Equation (2.2.7) and Equation (2.2.8)
K	-	geometric function
k	-	absorption index
N	-	number of elements
n	-	refractive index
$\tilde{n}$	-	complex index of refraction
$q''(x_i)$	-	net radiant heat loss at x_i per unit time and area
$S(x_i)$	-	direct solar illumination at x_i
$T(x_i)$	-	temperature at x_i
T_{ref}	-	reference temperature
α	-	parameter as defined in Equation (2.5.3)
β	-	parameter as defined in Equation (2.5.3)
β_{ia}, β_{ib}	-	dimensionless radiosities
Δ	-	length of each plate element
γ	-	opening angle

γ - parameter as defined in Equation (2.5.3)

ϵ - emissivity

ρ - directional reflectivity for unpolarized radiation

ρ_i - directional reflectivity for radiation polarized perpendicular to plane of incidence

ρ_s - directional reflectivity for radiation polarized parallel to plane of incidence

$\rho(I, J, M)$ - bi-directional reflectance of element I for energy incident from the source J and reflected to the receiving element M

ξ - dimensionless parameter

η - dimensionless parameter

ψ - polar angle of incidence

θ - polar angle of reflectance

θ_s - direction of solar field

σ - Stefan-Boltzmann constant

$\tilde{\sigma}$ - rms height of roughness elements

Subscripts

λ - monochromatic quantity

b - black

H - hemispherical

I - reflecting element

i - plate i

J - source element

j - plate j

M - receiving element

N - normal

1. OBJECTIVES AND SCOPE

Analysis is in progress to assess the importance of such real surface radiating characteristics as non-diffuseness and non-grayness on the radiant heat transfer of surfaces in a space environment. Section 2.1 reports the status of the non-gray, non-diffuse analysis for a simple system of surfaces. An analysis and preliminary results for equilibrium temperatures using gray diffuse theory is presented in Section 2.2 for the system under study. Section 2.3 reports the status of an analysis accounting for directional dependence of radiation properties. Some of the results reported in [2] for the bi-directional reflectance model are in error as discussed in Section 2.4. Criteria are being developed for the use of certain directional reflectance relations as reported in Section 2.5.

2. CURRENT STATUS

2.1 Radiant Heat Exchange For Non-Gray, Non-Diffuse Surfaces in a Space Environment

The equations governing the spectral intensity distribution for the thin strips geometry of Figure 1 have been formulated and coded for solution on the computer. An iterative method of solution is being attempted utilizing a finite difference approach in which each strip is subdivided into N equal length elements. The intensity in a selected direction is assumed uniform over the extent of each element. Solution for the radiant intensity requires preliminary calculation of $2N^3$ coefficients, $C_\lambda(I, J, M)$, given by

$$C_\lambda(I, J, M) = \int_{\eta_J - \frac{\Delta}{2}}^{\eta_J + \frac{\Delta}{2}} \rho_\lambda(I, J, M)\, K(I, J)\, d\,\eta_J \qquad (2.1.1)$$

where Δ denotes the length of each plate element. The arguments of C_λ can be defined with the aid of Figure 2. The first argument, I, refers to the reflecting element, the second, J, to the source of the incident ray, and the third, M, to the receiving element. The indicated integration is effectively over all angles of incidence. The bi-directional reflectance $\rho_\lambda(I, J, M)$ is that derived by Beckmann [1] and discussed in [2]. K(I, J) is a purely geometrical factor accounting for the orientation of the elements designated I and J. The Beckmann bi-directional reflectance model is an infinite series whose rate of convergence depends strongly on the polar angles of incidence and reflection as well as on the surface roughness parameters $\frac{\sigma}{\lambda}$ and $\frac{a}{\lambda}$. Limited calculations with a recently developed computer code indicated that an excessive amount of computer time is required to evaluate the coefficients with this code. Present efforts are directed toward the development of a more efficient code to decrease the computation time.

The result of the finite difference approach is a system of $2N^2$ simultaneous linear algebraic equations for the directional intensities. Matrix inversion codes are available to solve these equations. The solution procedure contemplated consists of determining a solution for a small number of elements on each plate and then successively increasing the number until convergence is achieved.

The solution techniques and computer codes developed for the

strip system require only minor modifications for application to the originally proposed system shown in Figure 3.

2.2 Radiant Heat Exchange for Gray Diffuse Surfaces in a Space Environment.

To assess the accuracy of gray diffuse theory in predicting radiant heat exchange and surface temperatures for engineering materials in a space environment requires a comparison of results from such analysis to that of the real surface analysis in progress. Unfortunately, sufficient results of gray diffuse analyses are not available for the system and associated environment under study. As a result of this deficiency, an effort was initiated to supplement the available results with those required for this study.

The system of two infinite width opaque planes of equal length oriented as shown in Figure 3 is considered. Energy exchange occurs only by radiant transport with all intervening media non-participating. Radiant properties of each surface are taken independent of wave length (gray), diffuse, and uniform. Either the temperature distribution or local radiant heat loss rate is specified on the surfaces; both are assumed independent of the direction normal to the figure. When the surface temperature distribution on the surfaces is specified, interest lies in the evaluation of local radiant heat transfer. On the other hand, for specified local radiant heat loss on the surfaces, the local temperature is required. In the latter case, equilibrium temperatures may be determined for zero local radiant heat transfer.

An analysis is briefly described which reduces the evaluation of local radiant heat loss or temperature to the solution of two simultaneous

linear integral equations which depend on numerous geometrical parameters. It is demonstrated that under certain conditions the governing integral equations may be reduced to two sets of independent integral equations, the solutions of which depend only on the surface properties and included angle. Equilibrium temperatures are presented for the adjoint plate system when fully illuminated by the solar field. These results are compared with those recently reported [3].

ANALYSIS

Consider first the evaluation of local radiant heat loss for the surfaces when the temperature distribution on each is specified. Because the properties of each plate are uniform and the temperature distribution dependent only on distance normal to the common apex, the spatial variation of local radiant heat loss depends only on the distance measured in the direction of plate length. The steady radiant transfer rate from an element dA_i of plate i is the difference between the rates at which energy is emitted and incident energy absorbed. On a unit area basis, the net radiant heat loss per unit time of the considered element, q_i'', may be expressed as

$$q_i''(x_i) = \frac{\epsilon_i}{1-\epsilon_i}\left[E_{b,i}(x_i) - B_i(x_i)\right], \quad (i = 1,2) \qquad (2.2.1)$$

where $E_{b,i}$, B_i, ϵ_i represent local black body emissive power, radiosity, and emissivity, respectively.

If the local radiant heat loss is specified, Eqn. (2.2.1) may be rearranged to yield the local temperature.

$$\sigma T_i(x_i)^4 = \left(\frac{1-\epsilon_i}{\epsilon_i}\right) q_i''(x_i) + B_i(x_i) \qquad (i = 1,2) \qquad (2.2.2)$$

In Eqn. (2.2.2), σ is the Stefan-Boltzmann constant.

In either situation, that is, specified temperature or specified heat flux, the evaluation of the quantity of interest (heat flux or temperature) is readily calculated once the radiosity distribution has been evaluated. With this in mind, attention is turned to the determination of the radiosity.

The radiosity of an element of surface i, $B_i(x_i)$, is the sum of the rate of emission and rate at which incident radiant energy is reflected. The incident energy consists of the sum of contributions due to diffuse energy leaving plate $j(j \neq i)$ and direct illumination by the collimated solar field. Thus,

$$B_i(x_i) = \epsilon_i E_{b,i}(x_i) + (1 - \epsilon_i)\left[\int_j B_j(x_j) K(x_i, x_j)\, dx_j + S_i(x_i)\right], \quad \begin{pmatrix} i = 1,2 \\ j = 1,2 \end{pmatrix} \; i \neq j \qquad (2.2.3)$$

where

$$K(x_i, x_j) = \frac{\sin^2 \gamma}{2} \frac{x_i x_j}{[x_i^2 + x_j^2 - 2 x_i x_j \cos \gamma]^{3/2}} \qquad (2.2.4)$$

The integral appearing in Eqn. (2.2.3) represents the contribution of the adjacent plate to the incident energy and $S_i(x_i)$ the direct illumination due to the solar field. The direct solar illumination for a selected element on plate i takes on various forms depending on the relation between the opening angle (γ) and direction of solar field (θ_s).

For surfaces with specified radiant flux, Eqn. (2.2.2) may be used to eliminate $E_{b,i}$ ($= \sigma T_i^4$) in favor of the known flux $q_i''(x_i)$ to yield

$$B_i(x_i) = q_i''(x_i) + \left[\int_j B_j(x_j) K(x_i, x_j)\, dx_j + S_i(x_i)\right], \quad \begin{pmatrix} i = 1,2 \\ j = 1,2 \end{pmatrix} \; i \neq j \qquad (2.2.5)$$

Both pairs of integral equations, that is, those for specified temperature distribution (Eqn. (2.2.3)), and those for specified surface heat flux (Eqn. (2.2.5)), are included in the general form

$$B_i(x_i) = G_i(x_i) + C_i \int_j B_j(x_j)\, K(x_i, x_j)\, dx_j \,, \qquad \begin{pmatrix} i = 1,2 \\ j = 1,2 \end{pmatrix} \; i \neq j \qquad (2.2.6)$$

For surfaces with specified temperature distribution

$$C_i = 1 - \epsilon_i \,, \quad G_i(x_i) = \epsilon_i E_{b,i}(x_i) + C_i S_i(x_i) \,, \quad (i = 1,2) \qquad (2.2.7)$$

while for surfaces of specified local radiant heat loss

$$C_i = 1, \quad G_i(x_i) = q_i''(x_i) + S_i(x_i) \,, \quad (i = 1,2) \qquad (2.2.8)$$

The solution of the simultaneous linear integral equations, Eqn. (2.2.6), depends upon a number of parameters including the properties of the plates, included angle, solar field direction, and either the distribution of temperature or radiant heat transfer along the surfaces.

Considerable simplification may be realized in solving the system of Eqn. (2.2.6) when the functions G_i are non-zero constants. In particular, it may be shown that the radiosities B_i are given by

$$B_i(x_i) = G_i\, \beta_{ia}(\xi_i) + G_j\, \beta_{ib}(\xi_i) \,, \qquad \begin{pmatrix} i = 1,2 \\ j = 1,2 \end{pmatrix} \; i \neq j \qquad (2.2.9)$$

where the dimensionless radiosities β_{ia} and β_{jb} are determined by the simultaneous integral equations

$$\begin{aligned} \beta_{ia}(\xi_i) &= 1 + C_i \int_{\xi_j} \beta_{jb}(\xi_j)\, K(\xi_i, \xi_j)\, d\xi_j \\ \beta_{jb}(\xi_j) &= C_j \int_{\xi_i} \beta_{ia}(\xi_i)\, K(\xi_i, \xi_j)\, d\xi_i \end{aligned} \qquad \begin{pmatrix} i = 1,2 \\ j = 1,2 \end{pmatrix} \; i \neq j \qquad (2.2.10)$$

The solution of Eqns. (2.2.10) depends only on the included angle and properties of the plates. For surfaces with specified radiant heat flux, the parameter dependence reduces to only the included angle.

The simplifications which result when the G_i are non-zero constants pertain to some important situations. The directly incident solar radiation is uniform for a fully illuminated system and a semi-illuminated system in which one surface is completely illuminated and the other receives no direct solar illumination. Of course, the trivial case of no direct illumination is also a possibility. For these conditions of exposure to the solar field, the G_i are constant provided the surface temperatures or radiant heat transfer is uniform. Equilibrium temperatures may be determined in the latter case only for fully illuminated surfaces.

In summary, when both surfaces have uniform but not necessarily identical temperatures and are exposed to the collimated solar field such that the system is fully- or semi-illuminated, the dimensionless local radiant heat loss of either surface may be evaluated from the relation

$$\frac{q_i''(x_i)}{\epsilon_i \sigma T_{ref}^4} = \frac{1}{(1-\epsilon_i)}\left[\left(\frac{T_i}{T_{ref}}\right)^4 - \left\langle\left(\frac{T_i}{T_{ref}}\right)^4 + (1-\epsilon_i)\frac{S_i}{\sigma T_{ref}^4}\right\rangle \beta_{ia} - \left\langle\left(\frac{T_j}{T_{ref}}\right)^4 + (1-\epsilon_j)\frac{S_j}{\sigma T_{ref}^4}\right\rangle \beta_{ib}\right] \qquad \left(\begin{matrix} i=1,2 \\ j=1,2 \end{matrix}\ i \neq j\right) \quad (2.2.11)$$

where T_{ref} is an arbitrary reference temperature. For surfaces of constant local radiant heat loss under the same conditions of solar illumination, the local temperature may be evaluated from the result

$$\left(\frac{T_i(x_i)}{T_{ref}}\right)^4 = \left(\frac{1-\epsilon_i}{\epsilon_i}\right)\left(\frac{q_i''}{\sigma T_{ref}^4}\right) + \left\langle\left(\frac{q_i''}{\sigma T_{ref}^4}\right) + \left(\frac{S_i}{\sigma T_{ref}^4}\right)\right\rangle \beta_{ia} + \left\langle\left(\frac{q_j''}{\sigma T_{ref}^4}\right) + \left(\frac{S_j}{\sigma T_{ref}^4}\right)\right\rangle \beta_{ib} \qquad (2.2.12)$$

The dimensionless radiosities β_{ia} and β_{ib} $(i=1,2)$ are the solutions to Eqn. (2.2.10).

METHOD OF SOLUTION

Numerical solutions to Eqns. (2.2.10) have been determined by expressing the integrals in finite difference form. For sufficiently small increments, the radiosity may be taken as uniform over the extent of an increment enabling analytical evaluation of the resulting integral coefficients. The result of this procedure is a system of 2N simultaneous, linear, algebraic equations for the unknown radiosities when each plate is subdivided into N intervals. Results obtained for the radiosities using increasing values of N were compared and the solution accepted when further increases resulted in insignificant changes in the results. Numerical results for local and total radiant heat loss obtained in this manner were indistinguishable from those reported for the adjoint plate system with equal temperature plates and identical properties in the absence of solar illumination [4].

LOCAL EQUILIBRIUM TEMPERATURE RESULTS

Equilibrium temperatures have been determined for the adjoint plate system ($a_o = b_o = 0$) with identical property plates and the solar field directed parallel to the bisector of the included angle. In such a situation, the temperature distribution is identical on both surfaces and independent of the surface properties.

The equilibrium temperature distributions are shown in Figure 4 for included angles of 30°, 45°, 60°, 90°, 135°, and 180° for a solar constant value of 421.7 BTU/hr. ft^2. Although this value is not that generally accepted, its use allows a direct comparison to results

recently reported [3] which employed a non-gray diffuse analysis to the same system.

In general, the results are in agreement with the expected trends:

1. Maximum temperature occurs at the apex and decreases with increasing opening angle.
2. Temperature decreases monotonically from apex to edge with the extent of the variation increasing with diminishing values of opening angle.

A comparison of results to those reported by Plamondon and Landram [3] which accounted for wave length dependence of properties shows large differences in predicted temperatures. For an included angle of 30°, the gray results obtained here predicted temperatures which agree with the reported results for aluminum but exceeded those for a surface painted PV-100 white + black by 130° R. For 60° included angle, the gray results were 120°R higher for the painted surface and 100°R lower for the polished aluminum. Since the analyses were in all other respects identical, these discrepancies must be attributed to the influence of the wave length dependence of the surface radiation properties.

2.3 Radiant Heat Exchange Between Specularly Reflecting Surfaces with Direction Dependent Properties

A preprint of the paper, "Radiative Heat Exchange Between Specularly Reflecting Surfaces with Direction-Dependent Properties," which will be presented at and included in the Proceedings of the Third International Heat Transfer Conference and Exhibit in Chicago, Illinois, in August, 1966, is included in the Appendix.

2.4 Radiation Properties for Rough Surfaces of Conducting Materials

A coding error was discovered in the program for the integration over all reflection angles of the Beckmann bi-directional reflectance model after Status Report No. 2 [2] was submitted. This error influenced the results for $G = 4\pi^2(\frac{\tilde{\sigma}}{\lambda})^2 (\cos\theta + \cos\psi)^2$ less than unity. Calculations are in progress to correct the erroneously reported results. Preliminary results indicate that the Beckmann model satisfies the unit directional reflectance requirement for larger values of $\frac{\tilde{\sigma}}{\lambda}$ than reported and also that the departure of the directional reflectance from unity for $\frac{\tilde{\sigma}}{\lambda} \geq 0.08$ is less than reported. In effect, these corrections imply that the range of applicability of the model is larger than was originally reported.

2.5 Radiation Properties for Optically Smooth Plane Surfaces

By application of Maxwell's equations to the reflection of an electromagnetic wave incident at polar angle θ with the normal of an optically smooth plane surface, the following relations for directional reflectivity of a non-magnetic metal may be derived:

RADIATION POLARIZED PERPENDICULAR TO PLANE OF INCIDENCE

$$\rho_s = \frac{\cos^2\theta - 2n\alpha\cos\theta + n^2(1+k^2)\beta}{\cos^2\theta + 2n\alpha\cos\theta + n^2(1+k^2)\beta} \qquad (2.5.1)$$

RADIATION POLARIZED PARALLEL TO PLANE OF INCIDENCE

$$\rho_i = \frac{n^2(1+k^2)\cos^2\theta - 2n\gamma\cos\theta + \beta}{n^2(1+k^2)\cos^2\theta + 2n\gamma\cos\theta + \beta} \qquad (2.5.2)$$

with

$$\left.\begin{aligned}
\alpha^2 &= \frac{(1+k^2)}{2}\left[\left(\frac{1-k^2}{1+k^2}\right) + \beta - \left(\frac{\sin^2\theta}{n^2(1+k^2)}\right)\right] \\
\beta^2 &= \left[1 + \left(\frac{\sin^2\theta}{n^2(1+k^2)}\right)\right]^2 - \frac{4}{(1+k^2)}\left[\frac{\sin^2\theta}{n^2(1+k^2)}\right] \\
\gamma &= \frac{(1-k^2)}{(1+k^2)}\,\alpha + \frac{2k}{(1+k^2)}\sqrt{(1+k^2)\,\beta - \alpha^2}
\end{aligned}\right\} \qquad (2.5.3)$$

where the optical constants n and k specify the real and imaginary components of the complex index of refraction

$$\tilde{n} = n(1-ik) \qquad (2.5.4)$$

For unpolarized radiation

$$\rho = \frac{1}{2}(\rho_s + \rho_i) \qquad (2.5.5)$$

where ρ denotes the directional reflectivity for unpolarized radiation.

In effect, the reflectivity relations above are spectral values since the complex refractive index is, in general, a complicated function of wave length. Also, the above results are equally applicable to dielectric media for which the absorption index is zero.

The complicated character of the exact reflectivity relations has prompted the use of simpler approximate equations whenever possible. One simpler form can be derived when

$$n^2(1+k^2) \gg 1 \qquad (2.5.6)$$

for which the factors α, β, and γ are approximately unity. The resultant reflectivity expressions are:

RADIATION POLARIZED PERPENDICULAR TO PLANE OF INCIDENCE

$$\rho_s = \frac{(n - \cos\theta)^2 + n^2k^2}{(n + \cos\theta)^2 + n^2k^2} \qquad (2.5.7)$$

RADIATION POLARIZED PARALLEL TO PLANE OF INCIDENCE

$$\rho_i = \frac{\left(n - \frac{1}{\cos\theta}\right)^2 + n^2 k^2}{\left(n + \frac{1}{\cos\theta}\right)^2 + n^2 k^2} \tag{2.5.8}$$

In addition to the advantage gained purely by the simplicity of these relations, it may be shown that the above directional reflectivities may be analytically integrated over hemispherical space to yield relatively simple analytical expressions for hemispherical reflectivity or emissivity. According to Dunkle [5] the result for hemispherical emissivity is

$$\epsilon_H = 4n - 4n^2 \ln\left(\frac{1 + 2n + n^2(1+k^2)}{n^2(1+k^2)}\right) + \frac{4n^2(1-k^2)}{k} \tan^{-1}\left(\frac{k}{1+n(1+k^2)}\right)$$

$$+ \frac{4}{n(1+k^2)} - \frac{4 \ln(1+2n+n^2(1+k^2))}{n^2(1+k^2)^2}$$

$$+ \frac{4(1-k^2)}{n^2 k(1+k^2)^2} \tan^{-1}\left(\frac{nk}{n+1}\right) \tag{2.5.9}$$

The approximate relations yield the correct value for normal emissivity, that is,

$$\epsilon_N = \frac{4n}{1 + 2n + n^2(1+k^2)} \tag{2.5.10}$$

A limited effort is in progress to ascertain the range of validity of the approximate relations for evaluating the directional, normal, and hemispherical properties of optically smooth plane surfaces. Establishment of such criteria enables one to use the simpler reflectivity relations in the approximate method of accounting for the finite conductivity of real materials in the bi-directional reflectance model.

Results for normal and hemispherical emissivity have been obtained for a range of values of the refractive (n) and absorption (k)

indices. As noted previously, the approximate relations yield the correct value for normal emissivity. Figures 5 and 6 illustrate the results for refractive indices greater than and less than unity, respectively.

Of more interest is the comparison of results for hemispherical emissivity obtained by numerical integration of the exact relations and those calculated from Eqn. (2.5.9). The results are shown in Figures 7 and 8 as a function of the refractive index for a range of values for absorption index. For values of n and k greater than unity, the discrepancy between the hemispherical emissivity values is indistinguishable on Figure 7. Larger discrepancies occur for n greater than unity when k is less than unity. The maximum error of 9.6% occurs for n = 1 and k = 0.75. On the other hand, for refractive index less than unity, errors incurred by the use of Eqn. (2.5.9) can be very large when k is small. Fortunately, most materials with refractive indices less than unity possess large values for absorption index so that Eqn. (2.5.9) is again adequate except for n approaching zero. Quantitative criteria in terms of the range of n and k necessary to assure a specified percentage accuracy in the use of the simpler relations are being developed.

3. PROPOSED FUTURE RESEARCH

Future efforts will be concentrated on the determination of heat transfer rates and equilibrium temperature distribution results from the non-gray, non-diffuse analysis. Corrections to the erroneous

results given in [2] for the Beckmann bi-directional reflectance model will be completed. Related studies in progress such as those of Sections 2.2 and 2.5 will be continued.

4. REFERENCES

1. P. Beckmann and A. Spizzichino, "The Scattering of Electromagnectic Waves from Rough Surfaces," The Macmillan Company, New York, 1963.

2. R. G. Hering, "Theoretical Study of Radiant Heat Exchange for Non-Gray, Non-Diffuse Surfaces in a Space Environment," Semi-Annual Status Report No. 2, NASA Research Grant, No. NGR-14-005-036.

3. J. A. Plamondon and C. S. Landram, "Radiant Heat Transfer from Non-Gray Surfaces With External Radiation," AIAA, 3rd Aerospace Sciences Meeting, New York, New York, AIAA Paper No. 66-21.

4. E. M. Sparrow, J. L. Gregg, J. V. Szel, and P. Manos, "Analysis, Results, and Interpretation for Radiation Between Some Simply-Arranged Gray Surfaces," Journal of Heat Transfer, Trans. ASME, Series C, Vol. 83, 1961, pp 207-214.

5. R. V. Dunkle, "Emissivity and Inter-Reflection Relationships for Infinite Parallel Specular Surfaces," Symposium on Thermal Radiation of Solids, NASA SP-55, 1966, pp 39-44.

5. FIGURES

Fig. 1. Thin Strips Geometry

Fig. 2. Finite Difference Form of Thin Strips Geometry

Fig. 3. Geometry of Analysis

Fig. 4. Equilibrium Temperature Distribution for Adjoint Plate System - Gray Diffuse Theory

Fig. 5. Normal Emissivity ($N \geq 1.0$)

Fig. 6. Normal Emissivity ($N \leq 1.0$)

Fig. 7. Comparison of Exact and Approximate Results for Hemispherical Emissivity ($N \geq 1.0$)

Fig. 8. Comparison of Exact and Approximate Results for Hemispherical Emissivity ($N \leq 1.0$)

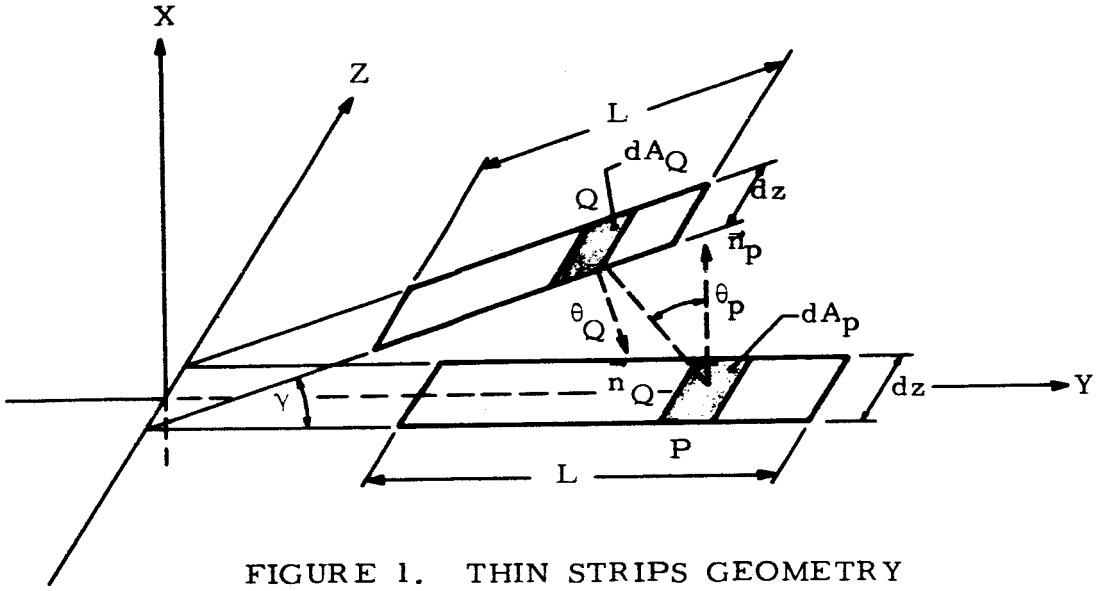

FIGURE 1. THIN STRIPS GEOMETRY

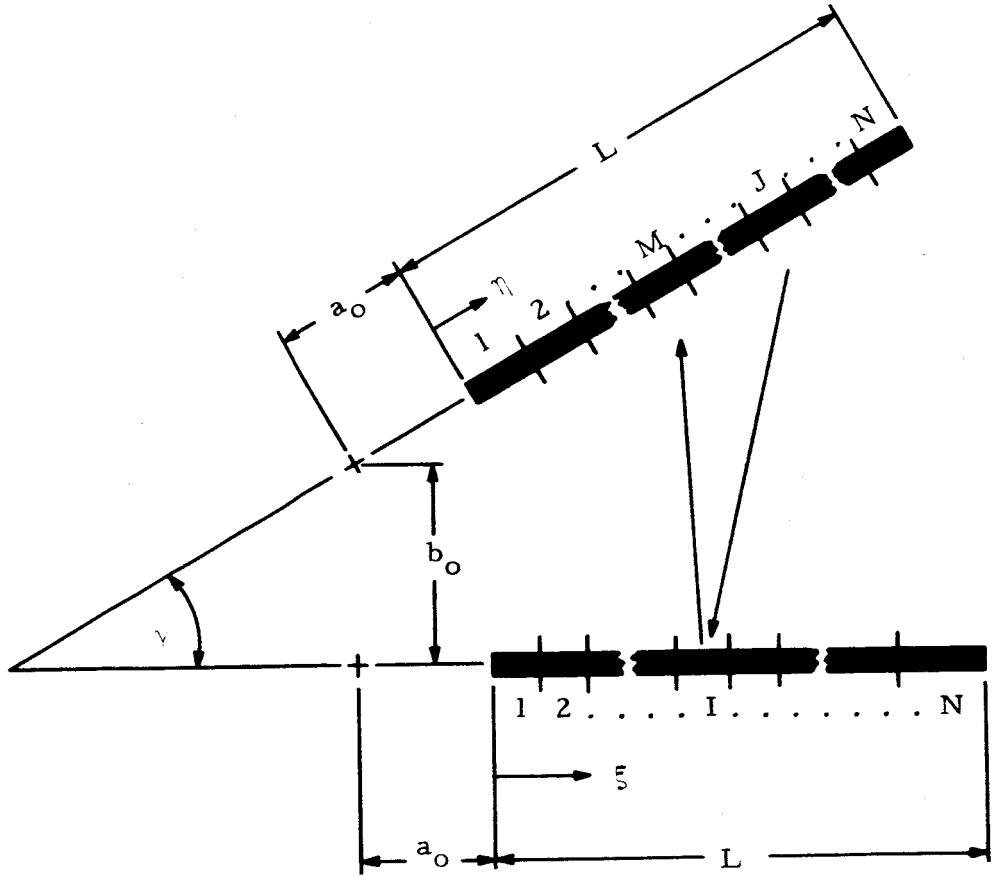

FIGURE 2. FINITE DIFFERENCE FORM OF THIN STRIPS GEOMETRY

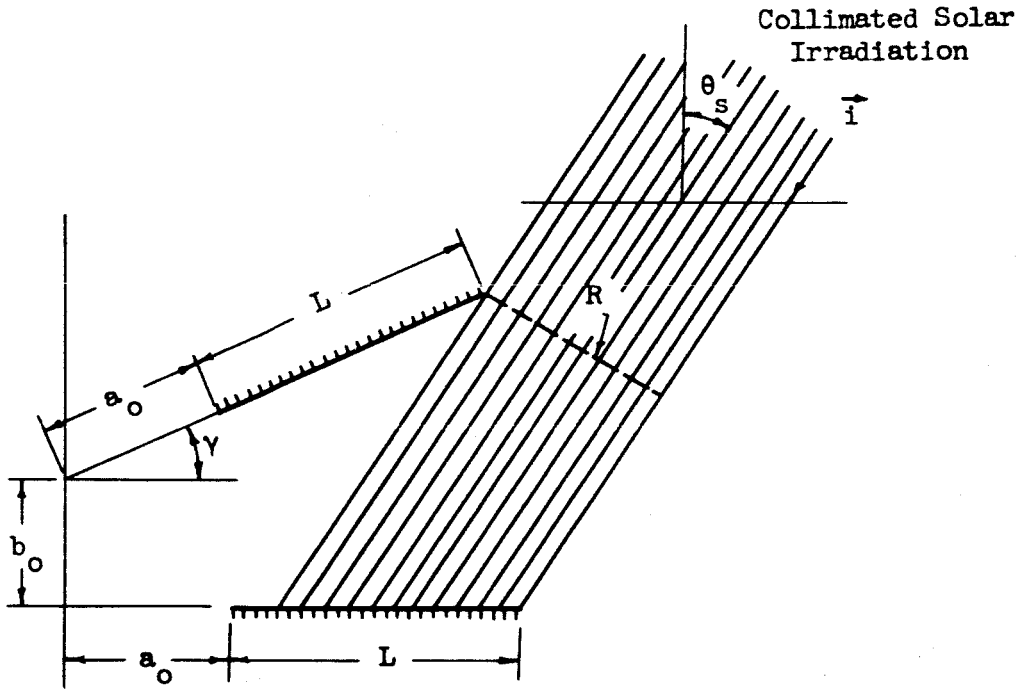

FIGURE 3.

GEOMETRY OF ANALYSIS

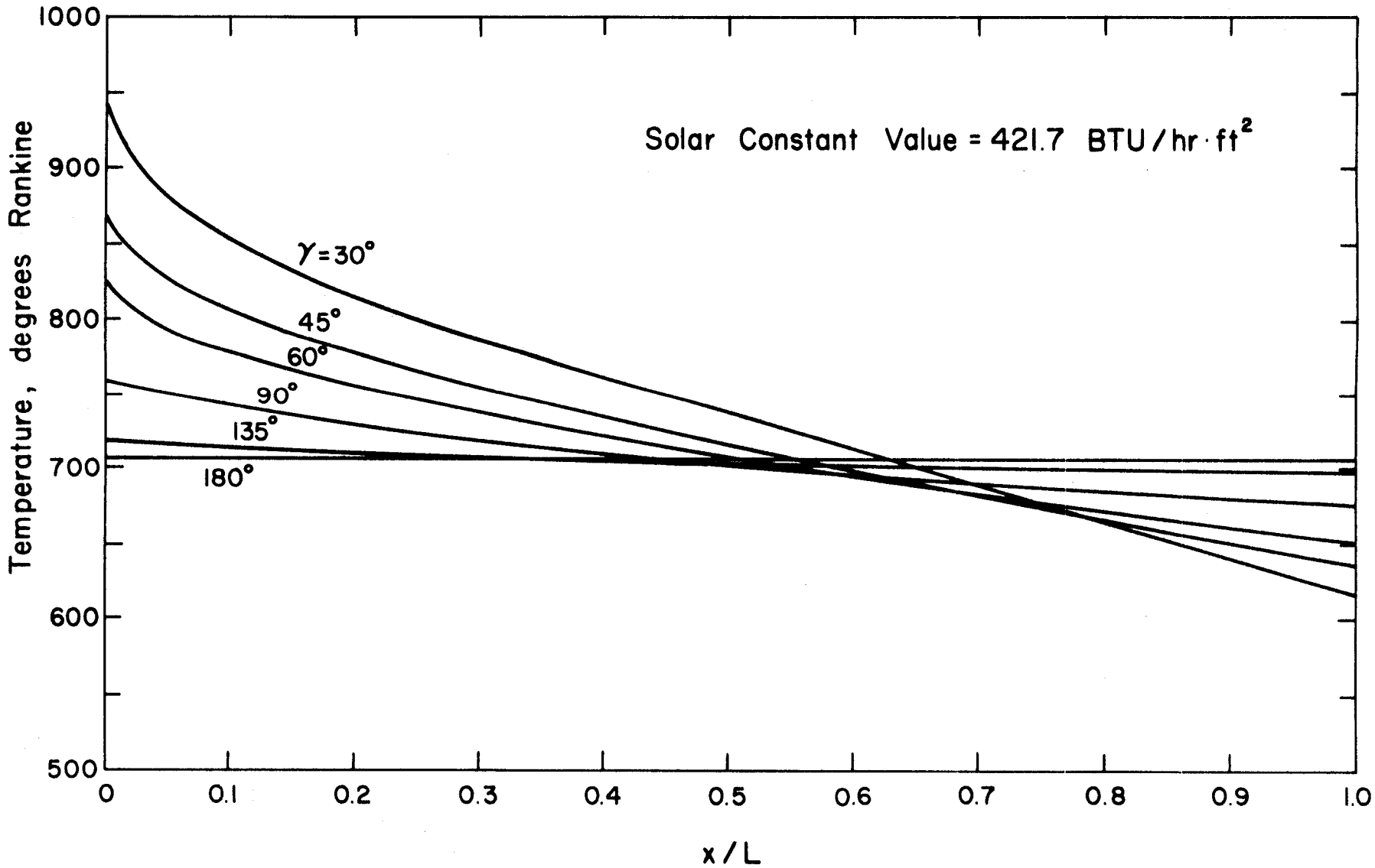

FIGURE 4. EQUILIBRIUM TEMPERATURE DISTRIBUTION FOR ADJOINT PLATE SYSTEM - GRAY DIFFUSE THEORY

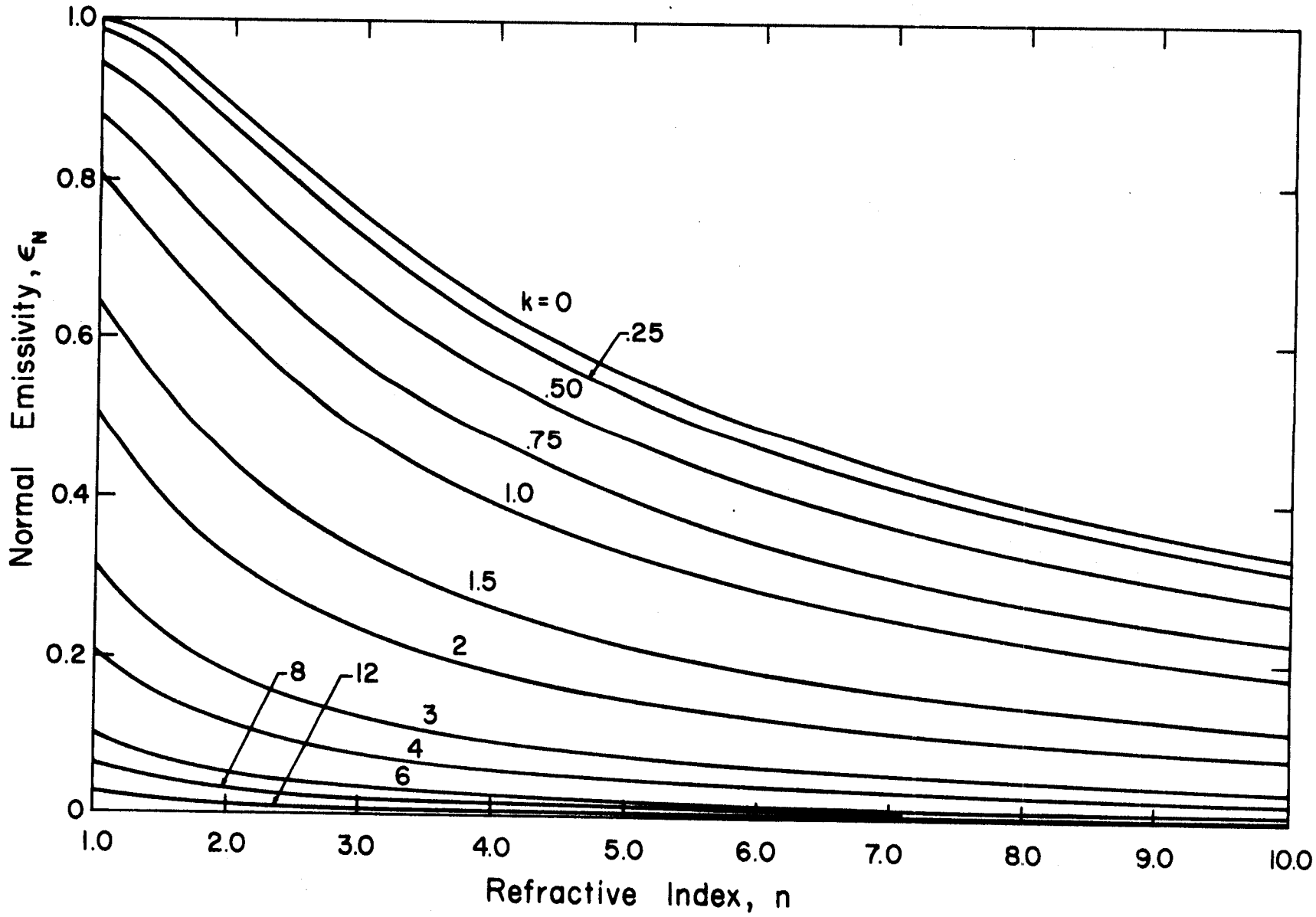

FIGURE 5. NORMAL EMISSIVITY ($N \geq 1.0$)

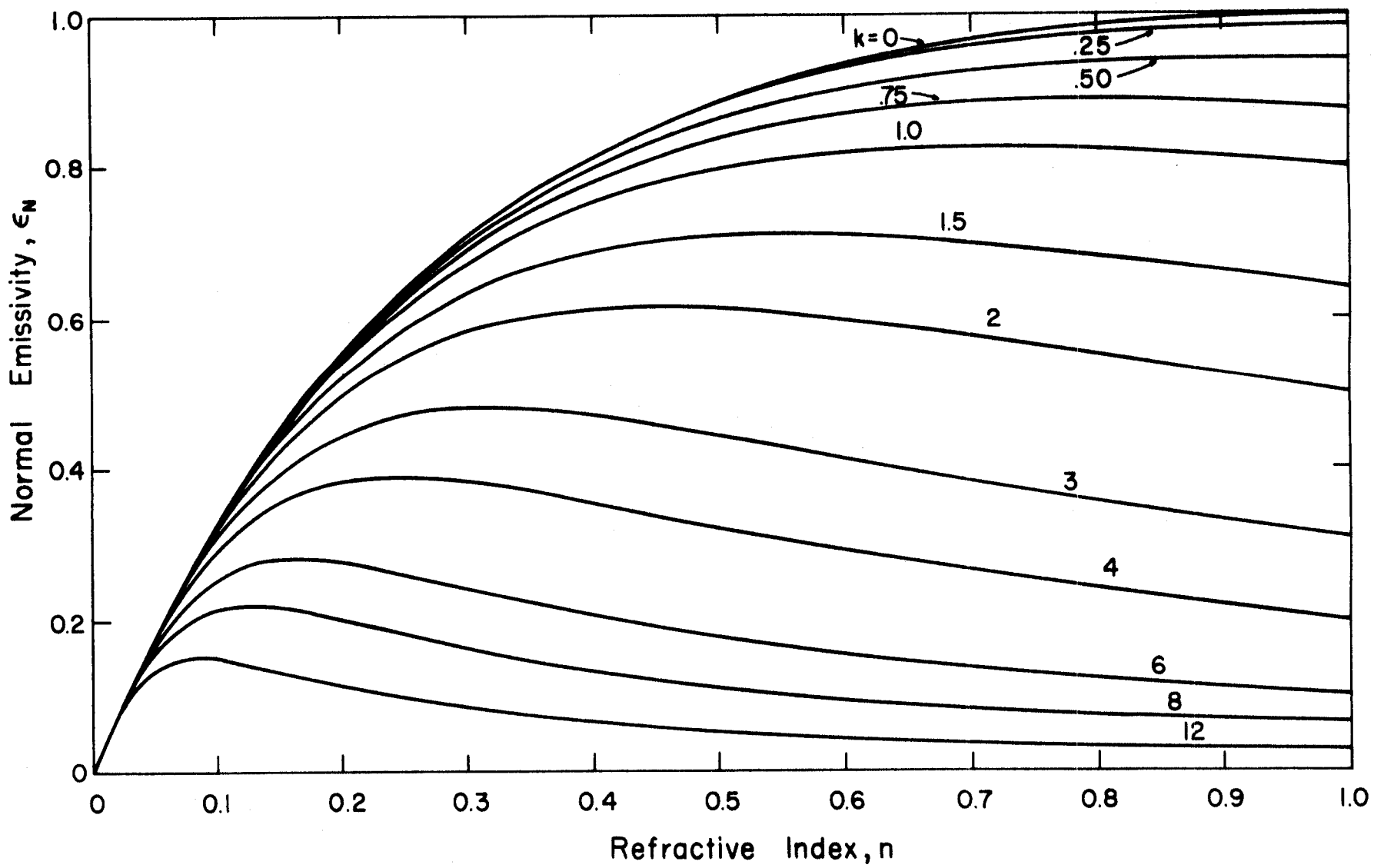

FIGURE 6. NORMAL EMISSIVITY (N ≤ 1.0)

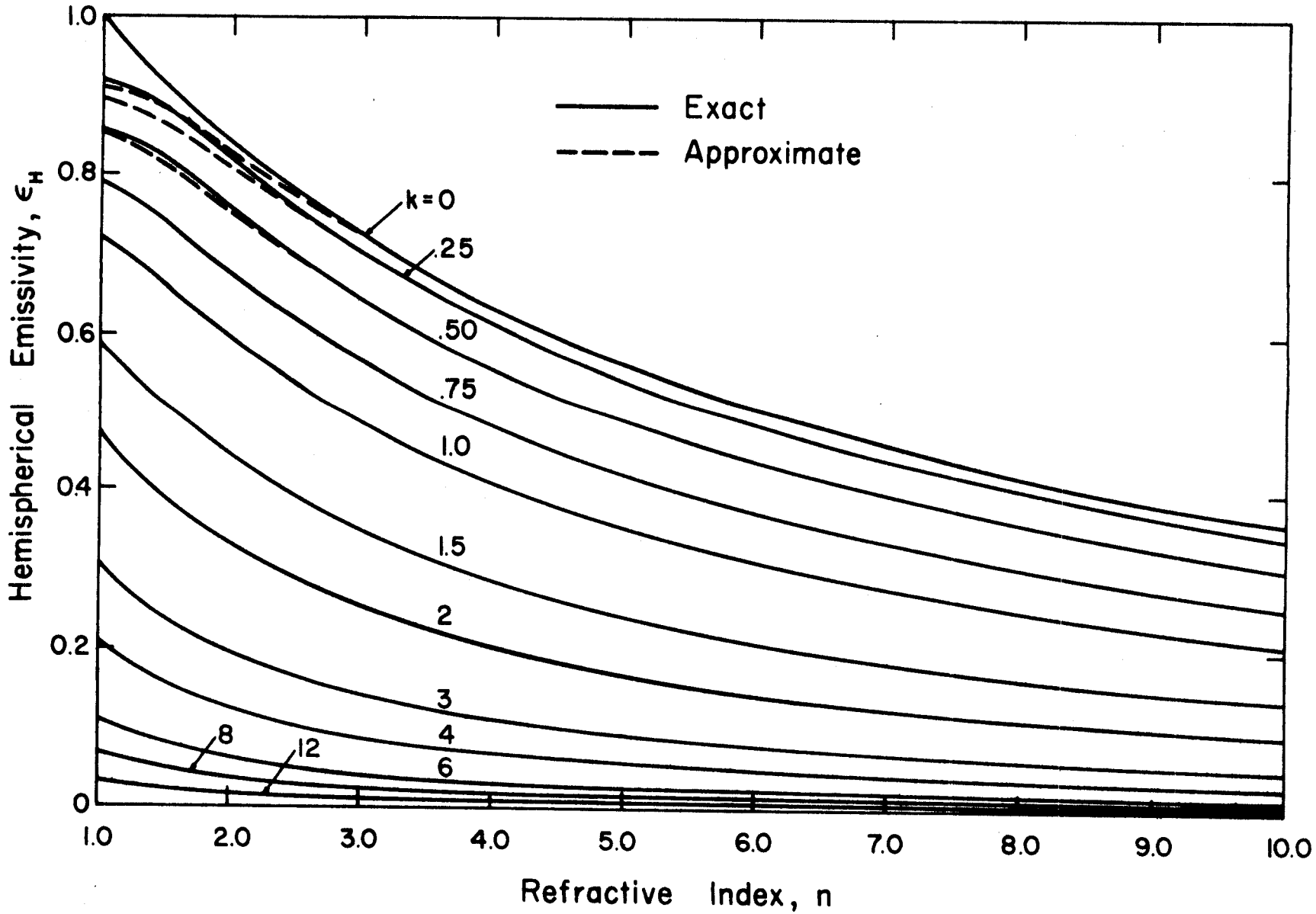

FIGURE 7. COMPARISON OF EXACT AND APPROXIMATE RESULTS FOR HEMISPHERICAL EMISSIVITY ($N \geq 1.0$)

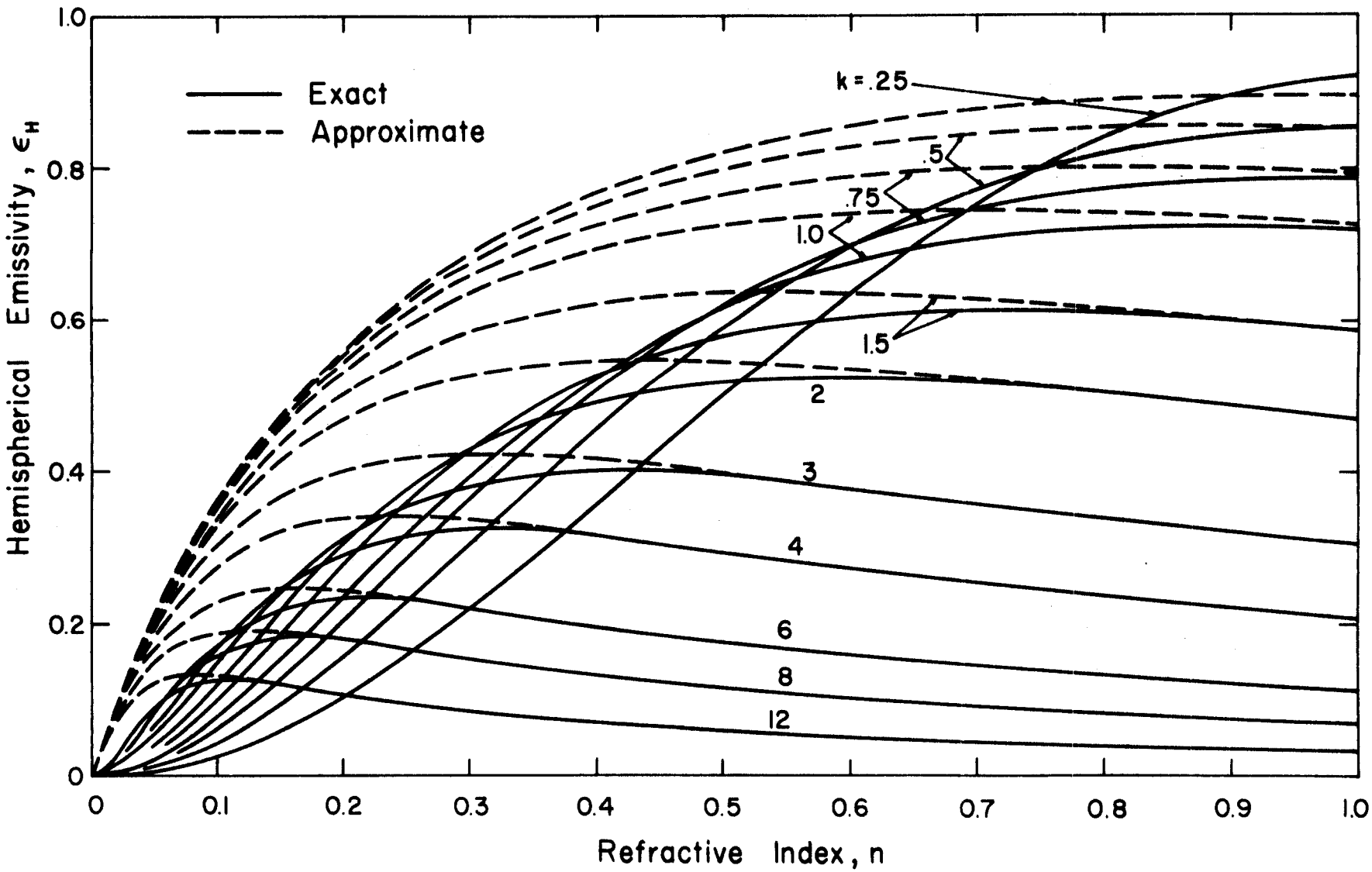

FIGURE 8. COMPARISON OF EXACT AND APPROXIMATE RESULTS FOR HEMISPHERICAL EMISSIVITY ($N \leq 1.0$)

6. APPENDIX - MANUSCRIPT OF TECHNICAL PAPER

RADIATIVE HEAT EXCHANGE BETWEEN SPECULARLY REFLECTING SURFACES WITH DIRECTION-DEPENDENT PROPERTIES

R. G. Hering
The University of Illinois
Urbana, Illinois

Abstract - An analysis is presented accounting for directional dependence of radiation properties on radiant heat transfer. The system studied is two equal-length plates sharing a common edge. The plates are gray specular reflectors with surface properties characterized by electromagnetic theory for smooth electrical conductors and non-conductors. Numerical results for local and total heat loss are presented for a range of included angles, plate temperature ratios, and hemispherical emissivity values. Local radiant-heat-loss calculations which neglect directional property characteristics can result in significant errors. Total surface heat loss is affected to a lesser degree by directional property variations.

Zusammenfassung - Die folgende Untersuchung zieht die Richtungsabhängigkeit der Strahlungseigenschaften von der Strahlungswärmeübertragung in Betracht. Die Versuchsanordnung besteht aus zwei Platten gleicher Länge, die eine Kante gemeinsam haben. Die Platten sind graue Speigelreflektoren, deren Oberflächeneigenschaften durch die elektromagnetische Theorie für glatte elektrische Leiter und Nichtleiter charakterisiert sind. Numerische Resultate für den örtlich beschränkten sowie auch den gesamten Wärmeverlust sind für eine Reihe von eingeschlossenen Winkeln, Verhältnissen von Plattentemperaturen und Halbkugelemissionszahlen angegeben. Berechnungen für örtlich beschränkte Wärmestrahlungsverluste, die Besonderheiten der richtungsbedingten Eigenschaften nicht in Betracht ziehen, führen zu fehlerhaften Ergebnissen. Der Gesamtwärmeverlust der Oberflächen ist zu einem geringeren Grad von den durch die Richtungseigenschaften eingeführten Abweichungen beeinflusst.

Резюме – В работе представлен анализ теплопередачи радиацией, в котором учтена способность излучения в зависимости от направления. Система, которая была подвержена изучению, состоит из двух одинаковой длины пластинок сходящихся под углом и касающихся друг друга одним краем. Пластинки имеют серые зеркально отражающие поверхности со свойствами которые характеризуются электро-магнитной теорией приложимой к электропроводникам и непроводникам. Также приведены цифровые данные подсчета локальной и общей потери тепла в пределах углов между пластинками, соотношений температур пластинок и значений полусферического излучения. Подсчет локальных потерь излучаемого тепла, в котором влияние направления на способность излучения пренебрегается, может привести к значительным ошибкам. Общая потеря тепла поверхностью подвержена в меньшей степени влиянию изменения способности излучения в зависимости от направления.

INTRODUCTION

Generally, the dependence of radiative surface properties on direction of incident or emitted radiation has been neglected in radiant heat transfer calculations. Possibly, this is a result of limited experimental data on directional property variations and to the computational difficulties introduced when these effects are considered in analysis. A common assumption is that emission is completely diffuse. Directional emittance measurements (1), however, indicate that surfaces deviate from the diffuse emission idealization. Further evidence is provided by the well-known fact (2) that the ratio of hemispherical to normal emittance is not unity, but usually about 1.2 for metals and 0.96 for non-metals. On the other hand, directional measurements (3) of specular reflectivity for smooth metallic and non-metallic surfaces generally confirm the results of electromagnetic theory (4). According to this theory the directional reflectivity is nearly independent of direction to values of about 50 degrees from the surface normal. For larger angles the reflectivity of metallic surfaces first diminishes rapidly, then increases sharply to unity at grazing incidence, whereas electrical non-conductors show a more gradual increase to unity.

The purpose of the present study is to include in analysis of radiant heat transfer the directional dependence of emissivity, absorptivity, and reflectivity for a system of specularly-reflecting surfaces. The results obtained can then be compared with those which neglect directional property variations and the importance of including such effects assessed. The relative significance of directional property variations for radiant transfer compared with other real-surface effects, such as departure from grayness and polarization, has not been clearly established. Approximate methods of analysis have been introduced recently (5, 6, 7) to account for the non-

diffuse character of real-surface reflectance in engineering calculations.

The system chosen for study is shown schematically in Figure 1 and represents two equal-length isothermal plane surfaces sharing a common edge. This configuration, which could represent a wedge cavity or successive elements in an array of longitudinal fins with high thermal conductivity, has received considerable attention. Analyses for diffuse emission and both limiting cases of diffuse (8) and specular (9) reflection have been reported. These studies consider identical gray surfaces at the same uniform temperature in the absence of external radiation fields. The analysis of reference (9), later used for comparison, neglected the directional dependence of reflectance.

In the analysis, certain simplifying assumptions are employed to insure a minimum number of parameters and to facilitate direct comparison with reported results. The surfaces are taken as indefinite in extent, and surface heat exchange occurs only by thermal radiation with incoming radiation from external sources considered negligible in comparison with energy emitted by the system. Each surface is gray, isothermal, and possesses uniform temperature-independent radiative properties. Temperatures and properties of the surfaces need not be identical. The surfaces are assumed to be specular reflectors of radiant energy with directional properties obeying the relations of electromagnetic theory. Polarization effects are neglected. The main interest lies in the local radiant heat loss on each of the surfaces and the total radiant energy transfer from the surfaces.

ANALYSIS

Local Radiant Heat Loss

Because each surface is isothermal and has uniform properties, the local rate of radiant energy loss on either plate depends spatially only on the distance measured normal to the common edge. For purposes of discussion, the surfaces are hereafter denoted as 1 and 2 according to Figure 1. Primed property values will refer to surface 2 and unprimed to surface 1. To evaluate the local heat loss, consider a typical surface element dA(=dxdy) of plate 1. The steady-state radiant transfer from this element, q_1, is the difference of the rates at which energy is emitted and incident energy absorbed. On a unit area basis, the net radiant transfer per unit time may be expressed as

$$q_1(x) = \epsilon_{H,1}\,\sigma T_1^4 - H_\gamma \qquad (1)$$

where H_γ represents the rate of absorption of incident energy. The subscript γ has been affixed to H to account for the different expressions required for the absorbed irradiation depending on the value of the opening angle. Attention is now turned to the evaluation of $H_\gamma(x)$.

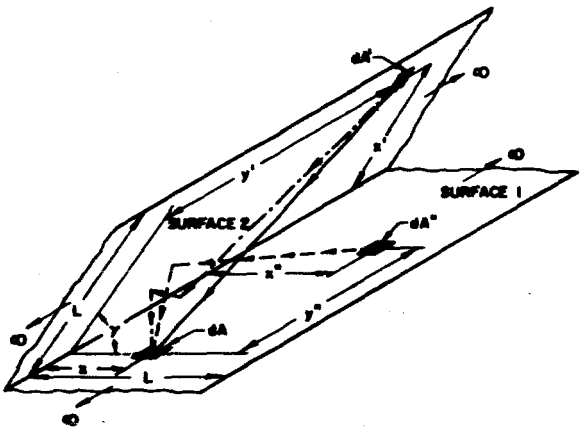

FIG. 1 ADJOINT PLATE SYSTEM

When the included angle is equal to or exceeds 180 deg, no interchange of radiant energy occurs between the surfaces. Then $H_\gamma \equiv 0$ and the local heat loss is uniform at a value dependent only on the hemispherical emissivity and temperature of the surface. For included angles in the range $90 \le \gamma < 180$ deg, the irradiation consists only of the direct transport of emission from the adjacent plate. All reflected energy passes out the opening. On the other hand, reflected energy must be accounted for in the evaluation of $H_\gamma(x)$ for opening angles less than 90 deg. The fundamental principle for evaluating the contribution of reflected energy to irradiation for specularly reflecting plane surfaces is given in reference(9). There it was observed that radiant energy reflected from a plane mirror appears to originate behind the mirror. Although this method has previously been applied only for direction independent properties, its use may be extended by properly accounting for the angular dependence of the properties. Expressions are presented for $90 \le \gamma < 180$ deg, $60 \le \gamma < 90$ deg, and $45 \le \gamma < 60$ deg although detailed analysis is limited to an opening angle of 45 deg.

To evaluate the emission of the adjacent plate directly transported to a typical surface element dA(=dx dy) of 1, consider first the element dA'(=dx'dy') of 2. Let $\theta_{a,\gamma}$ and $\theta_{e,\gamma}$ denote the angles determined by the ray of length r connecting the elements and the outward surface normals to the elements of 1 and 2, respectively. The rate of emission of dA' which is directly transported to and absorbed by dA per unit area of the absorbing element is

$$\alpha(\theta_{a,\gamma})\,\epsilon'(\theta_{e,\gamma})\,\sigma T_2^4\,\frac{\cos\theta_{e,\gamma}\cos\theta_{a,\gamma}}{\pi r^2}\,dx'dy' \qquad (2)$$

where $\alpha(\theta_{a,\gamma})$ and $\epsilon'(\theta_{e,\gamma})$ are the directional absorptivity of the absorbing element and directional emissivity of the emitting element evaluated at $\theta_{a,\gamma}$ and $\theta_{e,\gamma}$, respectively. The cosines of the angles $\theta_{e,\gamma}$ and $\theta_{a,\gamma}$ may be evaluated in terms of the coordinates as

$$\cos\theta_{e,\gamma} = x\sin\gamma/\sqrt{x^2+x'^2+y'^2-2xx'\cos\gamma}$$

$$\cos\theta_{a,\gamma} = x'\sin\gamma/\sqrt{x^2+x'^2+y'^2-2xx'\cos\gamma} \qquad (3)$$

To account for the contribution to the direct transport from all elements of 2 requires integration of equation (2). Thus

$$2\sigma T_2^4\int_0^L\int_0^\infty \epsilon_{a,\gamma}\epsilon'_{e,\gamma}\, d^2F_\gamma \qquad (4)$$

where

$$d^2F_\gamma = \frac{\sin^2\gamma}{\pi}\,\frac{xx'}{[x^2+x'^2+y'^2-2xx'\cos\gamma]^2}\,dx'dy' \qquad (5)$$

Azimuthal symmetry of the properties has been assumed in equation (4) and the gray body assumption employed to replace $\alpha(\theta_{a,\gamma})$ with $\epsilon(\theta_{a,\gamma})$. For brevity, the notation $\epsilon_{a,\gamma}$ for $\epsilon(\theta_{a,\gamma})$ and $\epsilon'_{e,\gamma}$ for $\epsilon'(\theta_{e,\gamma})$ has been introduced.

The surface element dA also receives emission from dA' in an indirect manner, such as by the dot-dashed path in Figure 1, undergoing two reflections before striking the element. For an observer at dA, this energy originates at the second image of dA' located on a surface inclined at an angle of 135 deg to surface 1. It is identical in amount to that which would be directly transported from this image, reduced in intensity by the product of the plate reflectivities evaluated at appropriate angles to account for the directional property variations. Thus the contribution of twice-reflected emission of dA' to the absorbed irradiation of dA is

$$\epsilon_{a,3\gamma}\epsilon'_{e,3\gamma}(1-\epsilon'_{r,22})(1-\epsilon_{r,12})\ \sigma T_2^4 d^2F_{3\gamma} \qquad (6)$$

where $d^2F_{3\gamma}$ is evaluated from equation (5) with γ replaced with 3γ(135 deg). Similarly $\epsilon_{a,3\gamma}$ and $\epsilon'_{e,3\gamma}$ are evaluated at the angles determined by equation (3) with γ replaced with 3γ. The gray opaque surface assumption has been used in equation (6) to exchange the reflectivities for $(1-\epsilon_{r,ij})$ where the subscripts i and j denote the ith reflection in a j reflection sequence. The cosines of the $\theta_{r,ij}$ at which the emissivities must be evaluated are as follows:

$$\cos\theta_{r,12} = \frac{(x\sin 2\gamma + x'\sin\gamma)}{\sqrt{x^2+x'^2+y'^2-2xx'\cos 3\gamma}}$$

$$\cos\theta_{r,22} = \frac{(x\sin\gamma + x'\sin 2\gamma)}{\sqrt{x^2+x'^2+y'^2-2xx'\cos 3\gamma}} \qquad (7)$$

Integration of (6) completes the determination of contributions to the absorbed irradiation of dA by reflected emission originating from 2.

$$2\sigma T_2^4\int_0^L\int_0^\infty \epsilon_{a,3\gamma}\epsilon'_{e,3\gamma}(1-\epsilon'_{r,22})(1-\epsilon_{r,12})d^2F_{3\gamma} \qquad (8)$$

The surface element dA also receives radiation emitted from elements on 1, say dA'', by the dashed path indicated in Figure 1; energy arrives at dA after a single specular reflection on 2. Again, for an observer located on dA, this energy originates at the first image of dA'' located on a plane inclined at 90 deg to plate 1. Its value is the product of the emission of dA'' directly transported from this image, reduced in magnitude by the reflectance of surface 2 evaluated for the direction of incidence. Thus the emission of dA'' which strikes dA after one reflection from 1 is

$$\epsilon_{a,2\gamma}\,\epsilon_{e,2\gamma}(1-\epsilon'_{r,11})\ \sigma T_1^4 d^2F_{2\gamma} \qquad (9)$$

where $d^2F_{2\gamma}$ is d^2F_γ of equation (5) with γ, x', and y' replaced with 2γ, x'', and y'' respectively. A similar exchange of variables in equation (3) determines the polar angles at which $\epsilon_{a,2\gamma}$ and $\epsilon_{e,2\gamma}$ are evaluated. The cosine of the angle $\theta_{r,11}$ at which $\epsilon'_{r,11}$ is evaluated is determined by the relation

$$\cos\theta_{r,11} = \frac{(x+x'')\sin\gamma}{\sqrt{x^2+x''^2+y''^2-2xx''\cos 2\gamma}} \qquad (10)$$

Since other images of 1 are not visible to an observer on 1, the reflected emission of surface 1 which contributes to the absorbed irradiation of dA is the integral of equation (9):

$$2\sigma T_1^4\int_0^L\int_0^\infty \epsilon_{a,2\gamma}\epsilon_{e,2\gamma}(1-\epsilon'_{r,11})d^2F_{2\gamma} \qquad (11)$$

Replacing the integration variables of equation (11) with x' and y' and subsequent summation of equations (4), (8), and (11) determines the absorbed irradiation $H_\gamma(x)$ as

$$H_\gamma(x) = 2\sigma\int_0^L\int_0^\infty\Big[\epsilon_{a,\gamma}\epsilon'_{e,\gamma}T_2^4 d^2F_\gamma + \epsilon_{a,2\gamma}\epsilon_{e,2\gamma}(1-\epsilon'_{r,11})T_1^4 d^2F_{2\gamma} + \epsilon_{a,3\gamma}\epsilon'_{e,3\gamma}(1-\epsilon_{r,12})(1-\epsilon'_{r,22})T_2^4 d^2F_{3\gamma}\Big] \qquad (12)$$

$$45\text{ deg} \le \gamma < 60\text{ deg}$$

Although derived for γ = 45 deg, the expression of equation (12) is valid for the full range of opening angles indicated. Similar analysis for opening angles in the range $60 \le \gamma < 90$ deg and $90 \le \gamma < 180$ deg results in parallel expressions for $H_\gamma(x)$. Introducing the dimensionless variables

$$R = (T_2/T_1)^4,\ \xi = x/L,\ \zeta = x'/L,\ \eta = y'/L \qquad (13)$$

into equation (12) and the results for other values of opening angle gives the following expression for the dimensionless local heat loss of surface 1:

$$\frac{q_1(\xi)}{\epsilon_{H,1}\sigma T_1^4} = 1 - \frac{2R}{\epsilon_{H,1}}\int_0^1\int_0^\infty G_\gamma(\xi,\zeta,\eta)\,d\zeta\,d\eta \qquad (14)$$

where

$$G_\gamma(\xi,\zeta,\eta) = \begin{cases} \epsilon_{a,\gamma}\epsilon'_{e,\gamma}f_\gamma, & 90 \le \gamma < 180\text{ deg} \\ \epsilon_{a,\gamma}\epsilon'_{e,\gamma}f_\gamma + \frac{1}{R}\epsilon_{a,2\gamma}\epsilon_{e,2\gamma}(1-\epsilon'_{r,11})f_{2\gamma}, & 60 \le \gamma < 90\text{ deg} \\ \epsilon_{a,\gamma}\epsilon'_{e,\gamma}f_\gamma + \frac{1}{R}\epsilon_{a,2\gamma}\epsilon_{e,2\gamma}(1-\epsilon'_{r,11})f_{2\gamma} + \epsilon_{a,3\gamma}\epsilon'_{e,3\gamma}(1-\epsilon_{r,12})(1-\epsilon'_{r,22})f_{3\gamma}, & 45 \le \gamma < 60\text{ deg} \end{cases} \qquad (15)$$

and

$$f_\gamma(\xi,\zeta,\eta) = \frac{\sin^2\gamma}{\pi}\,\frac{\xi\zeta}{[\xi^2+\zeta^2+\eta^2-2\xi\zeta\cos\gamma]^2} \qquad (16)$$

with

$$\left.\begin{aligned}
\cos\theta_{a,\gamma} &= \zeta\sin\gamma/\sqrt{\xi^2+\zeta^2+\eta^2-2\xi\zeta\cos\gamma}\\
\cos\theta_{e,\gamma} &= \xi\sin\gamma/\sqrt{\xi^2+\zeta^2+\eta^2-2\xi\zeta\cos\gamma}\\
\cos\theta_{r,11} &= (\xi+\zeta)\sin\gamma/\sqrt{\xi^2+\zeta^2+\eta^2-2\xi\zeta\cos 2\gamma}\\
\cos\theta_{r,12} &= (\xi\sin 2\gamma+\zeta\sin\gamma)/\sqrt{\xi^2+\zeta^2+\eta^2-2\xi\zeta\cos 3\gamma}\\
\cos\theta_{r,22} &= (\xi\sin\gamma+\zeta\sin 2\gamma)/\sqrt{\xi^2+\zeta^2+\eta^2-2\xi\zeta\cos 3\gamma}
\end{aligned}\right\} \quad (17)$$

In the form given in equation (14), local heat loss is expressed as a ratio to the maximum it could attain if the surface were radiating directly to an environment at a temperature of absolute zero. The departure of this ratio from unity represents the effect of the adjacent surface and of inter-reflections in obstructing the escape of radiation through the opening.

The local radiant heat loss of surface 2, $q_2/\epsilon_{H,2}\sigma T_2^4$, may be obtained from equation (14) by interchanging primed property values with unprimed and R with 1/R. Finally it can be demonstrated that for equal temperature surfaces of identical properties, equation (14) simplifies to the result of reference (9) when the angular variation of surface properties is ignored.

Total Heat Loss

Total heat transfer Q from each surface per unit width can be evaluated by integration of the local heat transfer over the plate surface. In dimensionless form, the total heat transfer of surface 1, Q_1, is

$$\frac{Q_1}{\sigma T_1^4 L} = \int_0^1 \left(\frac{q_1}{\sigma T_1^4}\right) d\xi \qquad (18)$$

where $q_1/\sigma T_1^4$ is available from equation (14) after multiplication by $\epsilon_{H,1}$.

DIRECTIONAL RADIATIVE PROPERTIES

The results of references (8, 9) are based on hemispherical emittance values of 0.9, 0.5, and 0.1. To facilitate direct comparison with these results, directional property distributions must be used which produce these hemispherical values when integrated over all directions. Electromagnetic theory (4) provides directional property relationships for optically smooth non-conductors and conductors of electricity in terms of the refractive and/or absorption index of the material. Because hemispherical properties are not generally available in terms of these material parameters, limited calculations were performed to ascertain the value of these parameters which result in the appropriate value of the hemispherical property.

For infra-red radiation non-conductors are characterized by large and conductors by small values of emittance. Therefore, directional distributions corresponding to dielectrics are employed for surfaces with hemispherical emissivities of 0.9 and 0.5 and a directional dependence characteristic of a metal for the hemispherical emissivity of 0.1. The values of the refractive index n which result in hemispherical emissivity values of 0.9 and 0.5 are 1.5565 and 6.1038 respectively. Although dielectrics do not have refractive indices as large as 6.1 in the infra-red, the directional emissivity exhibits characteristics intermediate to those of a dielectric and a conductor as would be expected for a material with a hemispherical emissivity of 0.5. Taking unity for the value of absorption index and assuming independence of refractive index with wave length, a value of 23.452 results for n of a metal. Directional emissivity distributions are shown in Figure 2.

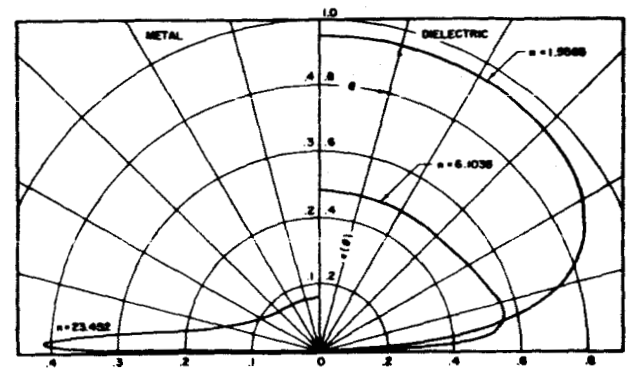

FIG. 2. THEORETICAL DIRECTIONAL EMISSIVITY DISTRIBUTIONS.

METHOD OF SOLUTION

Numerical solution of equation (14) was carried out on a digital computer using standard integration formulas. Accuracy of the calculations was verified by comparing numerical integration results for constant properties with the results calculated from the analytical relations of reference (9). In all cases, the numerical integration results for local and total heat loss differed from the analytical relations by less than 0.1 per cent. The results for directional properties are estimated to be of the same order of accuracy.

RESULTS

Local Heat Loss

Variation of the local radiant heat loss along the surfaces can be predicted qualitatively. Consider the dimensionless local heat loss of the surface designated 1 in Figure 1. According to equation (14), the variation of the heat loss is determined by the variation of the absorbed irradiation along the surface. Now the irradiation is greatest for surface elements located near the common edge and diminishes with distance measured normal to this edge. Further, the level and extent of variation of the incident energy increase with decreasing opening angle, increasing hemispherical emissivity of the adjacent surface, and increasing values of the emissive power ratio R. Thus, the dimensionless local heat loss should be

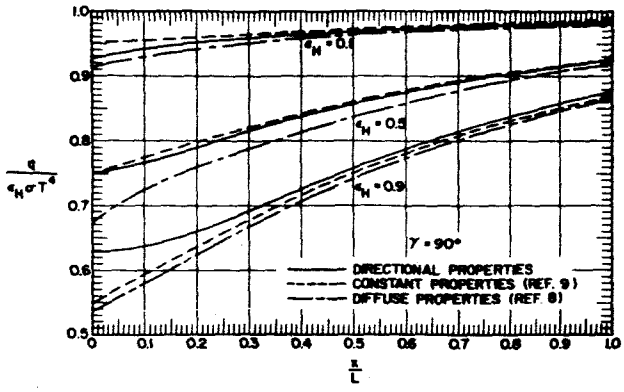

FIG. 3. LOCAL HEAT FLUX FOR $\gamma = 90°$

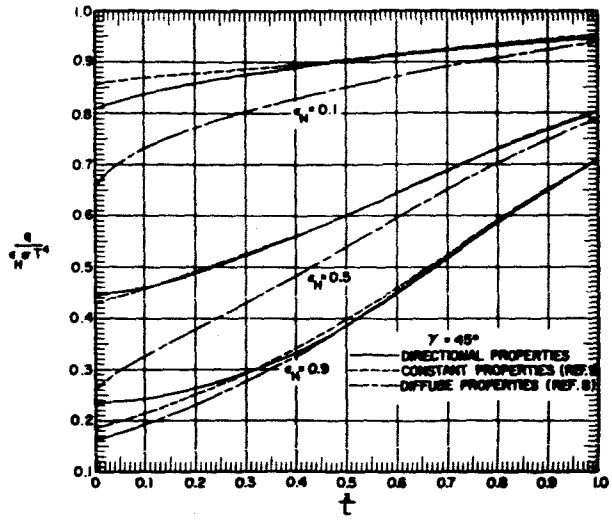

FIG. 4. LOCAL HEAT FLUX FOR $\gamma = 45°$.

expected to increase from a minimum value at the apex to a maximum value at the opposite end of the surface. This heat loss should exhibit an increase in magnitude and uniformity as the opening angle increases, as emissivity of the adjacent surface decreases, and as emissive power ratio diminishes. Directional property influences on local heat loss should be greatest for surface elements which receive major contributions to their irradiation from energy incident at grazing angles of incidence. Such elements are those located near the apex.

In general, the local heat loss distribution accounting for directional property variations are not expected to lie between the corresponding results of completely diffuse analysis or diffusely emitting-specularly reflecting analysis with constant properties. To facilitate later discussion, results of the foregoing analysis are denoted as DP (directional property) analysis, whereas results for diffusely emitting-specularly reflecting analysis with directionally independent properties are referred to as CP (constant property) analysis.

Representative results for local heat loss of equal-temperature surfaces with identical properties are displayed in Figures 3 and 4 for opening angles of 90 and 45 deg, respectively. Distributions are shown in each figure for hemispherical emissivity values of 0.1, 0.5, and 0.9. Also, for each value of emissivity, curves corresponding to results of diffuse analysis (8) and CP analysis (9) are included. It is observed that the calculated heat loss distributions confirm the earlier conclusions. The dimensionless heat loss monotonically increases from its value at the apex to a maximum at the end while its level and uniformity are greatest at the lowest emissivity and larger opening angle.

As expected, the largest differences between CP and DP analysis occur near the corner. For either opening angle, the heat loss results of CP analysis are generally high for the low emissivity surface and low for the high emissivity surface with the magnitude of this difference considerably greater for the high emissivity surface. The magnitude of the percent discrepancy increases with decreasing values of the opening angle attaining a maximum of approximately 20 per cent for $\epsilon_H = 0.9$ at $\gamma = 45$ deg.

It may also be noted that for $\gamma = 90$ deg, the heat loss results accounting for directional property variations exceed those of CP analysis over the extent of the plate for $\epsilon_H = 0.9$ and are everywhere less than CP results for $\epsilon_H = 0.1$. This is characteristic of the results when reflected energy is absent ($\gamma \geq 90$ deg) for surfaces of identical properties and may be readily explained in terms of the selected variations for the surface radiating properties. The CP results for $\epsilon_H = 0.5$ show good agreement with the DP results.

Figure 5 illustrates the influence of unequal surface temperatures for surfaces of identical radiation properties at a value of 90 deg for the opening angle. Local dimensionless heat loss distributions for the hemispherical emissivity values of 0.1, 0.5, and 0.9 are shown for both DP and CP analysis with R = 0.5, 1.0, and 2.0. In accordance with the earlier observations, the level of heat loss diminishes and becomes more non-uniform as the ratio of the emissive power of the adjacent surface increases relative to that of the considered surface. This effect is more pronounced for the higher emissivity surface.

The discrepancy between CP and DP results near the corner generally increases with R for a specified emissivity and opening angle. These differences generally are larger for the high emissivity surface and increase as the opening angle decreases. It may be noted that the heat loss result from CP analysis at the corner for R = 2.0 and $\epsilon_H = 0.9$ is less than one half of that obtained when account is taken of directional property variations. Again the results for CP analysis and $\epsilon_H = 0.5$ show good agreement with the results from DP analysis.

Local heat loss distributions representative of a system of surfaces with distinctly different directional property variations are presented in Figure 6 for an opening angle of 45 deg. The directional property dependence of the high emis-

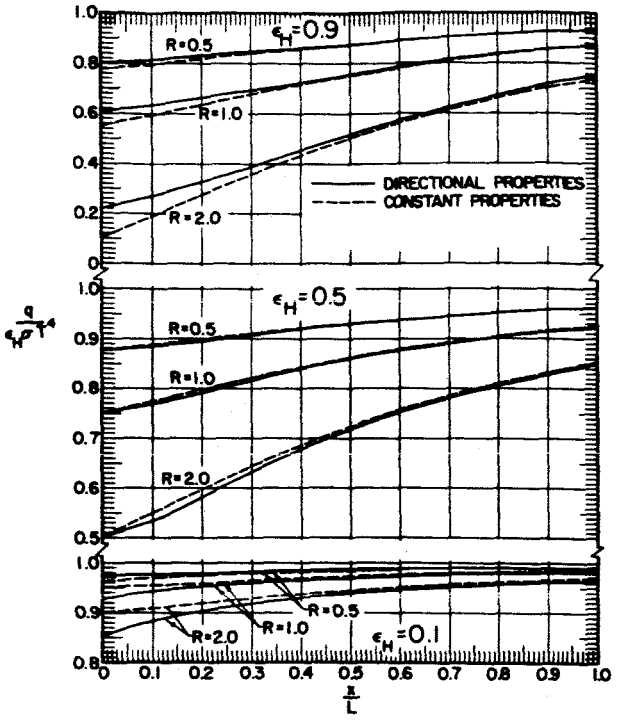

FIG. 5. LOCAL HEAT FLUX FOR $\gamma = 90°$ AND UNEQUAL PLATE TEMPERATURES.

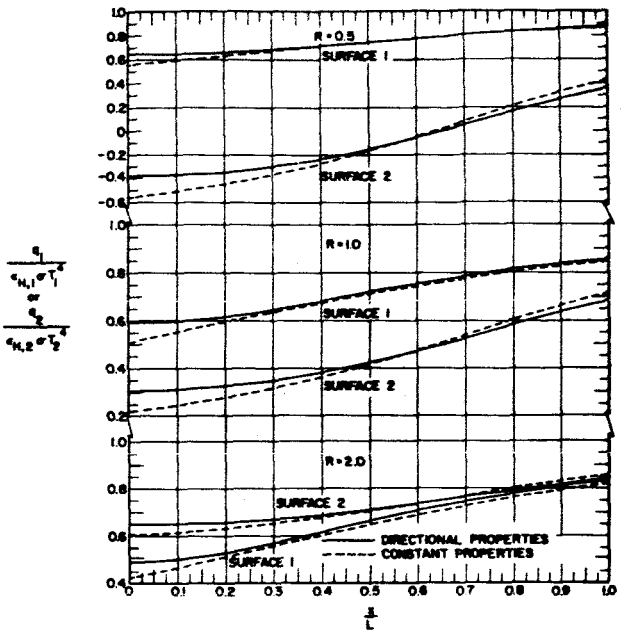

FIG. 6. LOCAL HEAT FLUX OF SURFACE 1 ($\epsilon_{H,1}$=0.9) AND SURFACE 2 ($\epsilon_{H,2}$=0.1) FOR $\gamma = 45°$

sivity surface is characteristic of an electrical non-conductor whereas that of the low emissivity surface is typical of metals. General trends noted previously for identical property surfaces are also apparent here. Compared to distributions for other values of opening angle and hemispherical emissivity, confirmation is provided for the earlier conclusions of increasing local heat loss and greater uniformity with increasing values of opening angle and diminishing emissivity of the adjacent plate. Again the difference between the results of CP and DP analysis are greatest at the corner. In contrast to the results of Figure 5, however, the greatest discrepancy between CP and DP analysis occurs for the low-emissivity surface. Results based on CP analysis exhibit a 50 per cent greater corner heat loss than DP analysis for R = 0.5.

Total Heat Loss

In Table 1, results obtained for total heat transfer of each surface per unit width are presented under the column heading DP. The corresponding results for constant properties listed under the columns headed CP extend those of (9).

Total heat transfer calculated on the basis of constant-property analysis generally shows exceptional agreement with that from directional property analysis. For identical property plates the discrepancy between CP and DP results is less than two per cent for the lower emissivity surfaces. Larger differences occur for the high emissivity surface, but are limited there to six per cent. CP analysis tends to yield slightly less heat loss for high-emissivity surfaces and slightly more for low-emissivity surfaces, with the per cent difference weakly influenced by the value for the opening angle.

CONCLUSIONS

Radiant heat transfer results obtained from analysis which accounts for the angular dependence of radiative surface properties for a system of specularly reflecting surfaces have been presented and compared with the corresponding results determined by analysis which neglects such property variations. For the range of system parameters studied, local heat transfer derived on the basis of constant property analysis with hemispherical property values gave results of acceptable engineering accuracy except near the corner, where discrepancies as large as a factor of two were observed. Total heat losses evaluated from the simpler constant property analysis were generally within a few per cent of those which account for directional property variations. It appears, therefore, that neglect of directional property variations in engineering radiant heat transfer calculations for specularly reflecting surfaces is generally justified. Care should be exercised, however, for surfaces which receive major contributions to their irradiation from energy incident at large angles relative to the surface normal.

ACKNOWLEDGMENTS

The author wishes to express his gratitude for the assistance of T. Smith, graduate assistant, who contributed both to the numerical computations and to the preparation of figures. The research was supported in part by National Aeronautics and Space Administration Grant NGR-14-005-036.

TABLE 1. TOTAL HEAT TRANSFER, $(Q/L)/\sigma T^4$

	Hem. Emiss.		Surface 1, $(Q_1/L)/(\sigma T_1^4)$						Surface 2, $(Q_2/L)/(\sigma T_2^4)$					
			R = 0.5		R = 1.0		R = 2.0		R = 2.0		R = 1.0		R = 0.5	
γ	ϵ_{H_1}	ϵ_{H_2}	D.P.	C.P.	D.P.	C.P.	D.P.	C.P.	D.P.	C.P.	D.P.	C.P.	D.P.	C.P.
135°	0.9	0.9	0.879	0.869	0.858	0.838	0.816	0.777	0.879	0.869	0.858	0.838	0.816	0.777
	0.9	0.5	0.885	0.883	0.870	0.866	0.840	0.831	0.440	0.431	0.470	0.466	0.485	0.483
	0.9	0.1	0.896	0.897	0.891	0.893	0.882	0.886	0.0821	0.0863	0.0911	0.0931	0.0955	0.0966
	0.5	0.5	0.489	0.490	0.479	0.481	0.458	0.462	0.489	0.490	0.479	0.481	0.458	0.462
	0.5	0.1	0.497	0.498	0.494	0.496	0.488	0.492	0.0878	0.0924	0.0939	0.0962	0.0969	0.0981
	0.1	0.1	0.0992	0.0996	0.0983	0.0992	0.0966	0.0985	0.0992	0.0996	0.0983	0.0992	0.0966	0.0985
90°	0.9	0.9	0.788	0.781	0.677	0.663	0.454	0.426	0.788	0.781	0.677	0.663	0.454	0.426
	0.9	0.5	0.835	0.834	0.770	0.768	0.640	0.636	0.241	0.236	0.370	0.368	0.435	0.434
	0.9	0.1	0.886	0.887	0.872	0.874	0.844	0.847	0.0440	0.0473	0.0720	0.0736	0.0860	0.0868
	0.5	0.5	0.462	0.463	0.425	0.427	0.350	0.354	0.462	0.463	0.425	0.427	0.350	0.354
	0.5	0.1	0.492	0.493	0.484	0.485	0.468	0.471	0.0677	0.0707	0.0838	0.0854	0.0919	0.0927
	0.1	0.1	0.0983	0.0985	0.0965	0.0971	0.0931	0.0941	0.0983	0.0985	0.0965	0.0971	0.0931	0.0941
60°	0.9	0.9	0.693	0.687	0.490	0.484	0.0844	0.0791	0.693	0.687	0.490	0.484	0.0844	0.0791
	0.9	0.5	0.743	0.733	0.630	0.621	0.405	0.396	0.0479	0.0467	0.273	0.272	0.385	0.384
	0.9	0.1	0.798	0.780	0.775	0.757	0.730	0.712	0.0101	0.0099	0.0550	0.0549	0.0774	0.0774
	0.5	0.5	0.419	0.421	0.356	0.358	0.231	0.233	0.419	0.421	0.356	0.358	0.231	0.233
	0.5	0.1	0.454	0.457	0.442	0.445	0.417	0.420	0.0489	0.0493	0.0739	0.0743	0.0864	0.0868
	0.1	0.1	0.0955	0.0963	0.0930	0.0938	0.0879	0.0888	0.0955	0.0963	0.0930	0.0938	0.0879	0.0888
45°	0.9	0.9	0.632	0.626	0.377	0.376	-0.132	-0.125	0.632	0.626	0.377	0.376	-0.132	-0.125
	0.9	0.5	0.650	0.642	0.510	0.502	0.230	0.222	-0.0642	-0.0663	0.216	0.213	0.355	0.353
	0.9	0.1	0.674	0.658	0.646	0.630	0.592	0.574	-0.0098	-0.0126	0.0450	0.0435	0.0724	0.0716
	0.5	0.5	0.383	0.384	0.304	0.304	0.145	0.145	0.383	0.384	0.0304	0.304	0.145	0.145
	0.5	0.1	0.416	0.418	0.400	0.402	0.367	0.369	0.0326	0.0334	0.0654	0.0660	0.0819	0.0822
	0.1	0.1	0.0932	0.0940	0.0895	0.0906	0.0822	0.0838	0.0932	0.0940	0.0895	0.0906	0.0822	0.0838

NOMENCLATURE

dA, dA', dA''	=	surface elements
f	=	function defined in equation (16)
F	=	function defined in equation (5)
G	=	function defined in equation (15)
H	=	absorbed irradiation
L	=	plate length
n	=	refractive index
q	=	local heat transfer rate per unit area
Q	=	total heat transfer rate per unit width
r	=	length of ray between elements
R	=	temperature ratio, $(T_2/T_1)^4$
x, x', y', x'', y''	=	coordinates
α	=	absorptivity
γ	=	opening angle
ϵ	=	emissivity
ζ	=	dimensionless coordinate, x'/L
η	=	dimensionless coordinate, y'/L
θ	=	polar angle
ξ	=	dimensionless coordinate, x/L
σ	=	Stefan-Boltzmann's constant

Subscripts

1	=	surface 1
2	=	surface 2
a	=	absorbing element
e	=	emitting element
H	=	hemispherical
r	=	reflecting element
γ	=	opening angle

REFERENCES

1. Abbott, G. L., "Total Normal and Total Hemispherical Emittance of Polished Metals," Measurement of Thermal Radiation Properties of Solids, Joseph C. Richmond, ed., NASA SP-31, 1963, pp 293-306.
2. Eckert, E.R.G. and Drake, R.M., Heat and Mass Transfer, McGraw-Hill Book Company, Inc., New York, N.Y., 1959.
3. Dunkle, R. V., Edwards, D. K., Gier, J. T., Nelson, K. E., Roddick, R. D., "Heated Cavity Reflectometer for Angular Reflectance Measurements," Progress in International Research on Thermodynamic and Transport Properties, Joseph F. Masi and Donald H. Tsai, ed., 1962, pp 541-562.
4. Ditchburn, R. W., Light, Interscience Publishers, Inc., New York, N.Y., 1963.
5. Bevans, J. T. and Edwards, D. K., "Radiation Exchange in an Enclosure With Directional Wall Properties," Journal of Heat Transfer, Trans. ASME, Series C, vol. 87, 1965, pp 388-396.
6. Sarofim, A. F. and Hottel, H. C., "Radiative Exchange Among Non-Lambert Surfaces," ASME paper No. 65-HT-7.
7. Sparrow, E. M. and Lin, S. L., "Radiation Heat Transfer at a Surface Having Both Specular and Diffuse Reflectance Components," Int. J. Heat Mass Transfer, vol 8, pp 769-779, 1965.
8. Sparrow, E. M., Gregg, J. L., Szel, J. V., Manos, P., "Analysis, Results, and Interpretation for Radiation Between Some Simply Arranged Gray Surfaces," Journal of Heat Transfer, Trans ASME, Series C, vol. 83, 1961, pp 207-214.
9. Eckert, E. R. G. and Sparrow, E. M., "Radiative Heat Exchange Between Surfaces With Specular Reflection," Int. J. Heat Mass Transfer, vol. 3, No. 1, 1961, pp 42-54.